NREL
NATIONAL RENEWABLE ENERGY LABORATORY

FAST Code Verification of Scaling Laws for DeepCwind Floating Wind System Tests

Preprint

Anant Jain
Intertek

Amy N. Robertson and Jason M. Jonkman
National Renewable Energy Laboratory

Andrew J. Goupee
University of Maine

Richard W. Kimball
Maine Maritime Academy

Andrew H. P. Swift
Texas Tech University

To be presented at the 22nd International Offshore and Polar Engineering Conference
Rhodes, Greece
June 17 – 22, 2012

Conference Paper
NREL/CP-5000-54221
April 2012

Contract No. DE-AC36-08GO28308

NOTICE

Available electronically at http://www.osti.gov/bridge

Available for a processing fee to U.S. Department of Energy
and its contractors, in paper, from:

U.S. Department of Energy
Office of Scientific and Technical Information

P.O. Box 62
Oak Ridge, TN 37831-0062
phone: 865.576.8401
fax: 865.576.5728
email: mailto:reports@adonis.osti.gov

Available for sale to the public, in paper, from:

U.S. Department of Commerce
National Technical Information Service
5285 Port Royal Road
Springfield, VA 22161
phone: 800.553.6847
fax: 703.605.6900
email: orders@ntis.fedworld.gov
online ordering: http://www.ntis.gov/help/ordermethods.aspx

Cover Photos: (left to right) PIX 16416, PIX 17423, PIX 16560, PIX 17613, PIX 17436, PIX 17721

Printed on paper containing at least 50% wastepaper, including 10% post consumer waste.

FAST Code Verification of Scaling Laws for DeepCwind Floating Wind System Tests

Anant Jain
Intertek
Louisville, Colorado, USA

Amy N. Robertson
National Renewable Energy Laboratory
Golden, Colorado, USA

Jason M. Jonkman
National Renewable Energy Laboratory
Golden, Colorado, USA

Andrew J. Goupee
University of Maine
Orono, Maine, USA

Richard W. Kimball
Maine Maritime Academy
Castine, Maine, USA

Andrew H. P. Swift
Texas Tech University
Lubbock, Texas, USA

ABSTRACT

This paper investigates scaling laws that were adopted for the DeepCwind project for testing three different floating wind systems at 1/50 scale in a wave tank under combined wind and wave loading. The 1/50 scaling of the full-scale 5-MW wind turbine system is performed based on Froude scaling laws, which are commonly used for offshore structures. The scaling approach adopted is verified through FAST, an aero-hydro-servo-elasto dynamic modeling tool, by comparing the consistency of simulation results between model and full scale. The Froude scaling approach does not maintain proper Reynolds number scaling and the implications of this issue are discussed.

KEYWORDS: Froude scaling; offshore floating wind turbine; NREL FAST; DeepCwind; model testing

NOMENCLATURE

C	= wave celerity
C_B	= frictional force coefficient for mooring line and sea floor
D	= diameter of the structure
E	= Young's modulus
$EI(z)$	= distributed structural rigidity
EA	= longitudinal axial stiffness
F_r	= Froude number
g	= acceleration due to gravity
H_F	= mooring line fairlead tension along horizontal axis
I	= moment of inertia
J	= mass moment of inertia
L	= unstretched length of mooring line
m	= mass of the structure
r	= distance between reference point and center of gravity
R	= radius of the rotor
Re	= Reynolds number
t	= time
TSR	= tip-speed ratio
u	= fluid velocity
$u(z,t)$	= out-of-plane deflection
V_F	= mooring line fairlead tension along vertical axis
V	= total wind speed
$x_F(H_F, V_F)$	= mooring line fairlead to anchor distance along horizontal axis
z	= radial location from center of the hub, to tip of the blade
z'	= dummy variable for integration
$z_F(H_F, V_F)$	= mooring line fairlead to anchor distance along vertical axis
Λ	= derived scaling factor
λ	= fundamental scaling factor (1/50)
α	= wind speed to wave celerity ratio
ν	= kinematic viscosity of the fluid
ω	= mass/length ratio of mooring line under water
Ω	= rotational speed
$\rho A(z)$	= distributed lineal density

INTRODUCTION

Model testing is used to facilitate technological advancement of systems, where prototype testing is not economically feasible. It is a proven methodology for research and development of ocean and offshore engineering systems, and is used to better understand the system dynamics and responses. To estimate the dynamic properties of a full-scale prototype, the empirical data from the model tests or simulations is scaled up by introducing fundamental and derived scaling laws. This paper discusses the implementation of a similar approach to better comprehend the dynamics of floating offshore wind systems through model testing. Though the testing of offshore structures and wind turbines at model scale has been used extensively, combining both systems in one test complicates the methodology of the commonly used scaling laws and introduces new terms.

The DeepCwind consortium is a group of academic and research organizations that share a common goal of advancing floating offshore wind development in the United States. The offshore wind energy research led by DeepCwind commenced with the 1/50-scale model testing of several 5-MW floating offshore wind turbines (FOWT) at the Maritime Research Institute Netherlands (MARIN). The model tests were conducted to identify the system response of three different design concepts of floating wind systems and to generate high-fidelity system response data needed to validate tools used for modeling these systems (De Ridder et. al., 2011). To perform the model tests, a set of scaling laws was developed to scale the 5-MW systems to a size that could be tested in the wave basin. To do this experiment, DeepCwind chose to

scale the geometry by a factor of λ = 1/50 by utilizing the proven technique of Froude scaling, typically used in the scaling of offshore structures. Others have approached the scaling of offshore wind systems for tank testing in a similar manner, including: the 1/67-scale model testing of a semi-submersible platform by Principle Power Inc. (Cermelli et. al., 2010), the 1/47-scale model testing of a spar-buoy platform by Hydro Oil and Energy (Skaare et. al., 2007), and the scale model testing of a semi-submersible platform (supporting three wind turbines) by WindSea (WindSea, 2006-2010). But, none gave a full description of the scaling laws used, nor did they attempt to verify the appropriateness of the scaling laws.

The aim of this paper is to verify the consistency of the scaling laws adopted by the DeepCwind consortium for the scaled testing of FOWTs. The comparison was accomplished using the simulation tool FAST (Jonkman et al, 2005) by comparing system responses between a full-scale and a model-scale system, to verify that the results scaled in a manner consistent with the scaling of the system parameters. This consistency is important to show that simulation results at full scale can be directly compared to upscaled test results from the wave basin. Such a study was deemed necessary because (1) the scaling approach was new and had not previously been tested to the author's knowledge (and was initially questioned) and (2) there are many nonlinearities and coupled physics in the equations of system dynamics used in the FAST code, which is a complex aero-hydro-servo-elasto dynamic modeling tool. It could be circumstantially anticipated that the numerical simulation of system responses between a full-scale and model-scale system would be consistent, but we wanted to be prudent and verify this before accepting it in faith. The project also enabled us to develop a tool that can quickly adapt full-scale inputs/outputs to inputs/outputs at model scale, or vice versa.

We investigated the scaling laws using two floating offshore wind turbine models, a modified version of the Offshore Code Comparison Collaboration (OC3)-Hywind spar-buoy (Jonkman, 2009a), and the Massachusetts Institute of Technology/National Renewable Energy Laboratory (MIT/NREL) tension-leg platform (TLP) (Matha, 2010). These models were not the exact ones tested in the wave basin, but were sufficient for examining the validity of the scaling approach used for the DeepCwind model tests.

One of the most significant weaknesses in using a Froude-based scaling approach is the inconsistency in the scaling of Reynolds number. This is a known issue that must be investigated. This issue will be discussed later in the paper, but for now, we put this issue aside to investigate the scaling laws independent of this factor.

After verifying the scaling laws and showing the validity of comparing full-scale simulations to upscaled tank test results, the next step of this work is to create and tune the models of the FOWTs in FAST to produce results similar to those seen in the tank. This work is on-going, and preliminary results can be found in Stewart et. al., 2012.

SCALING LAWS AND SCALED INPUT PARAMETERS

The DeepCwind scaling laws are based on three non-dimensional quantities: Froude number, tip-speed ratio, and the ratio of wind speed to wave celerity. Froude scaling is the most preferred scaling technique used for model testing of offshore structures. Froude number consistency between full-scale and model-scale levels is based on geometric scaling and is derived from the dimensional units of the quantities to be scaled (Martin, 2011; Chakrabarti, 2008). It is important to note that maintaining the tip-speed ratio and wind speed to wave celerity ratio between scales is entirely consistent with Froude scaling. The reason to use these ratios is to extend the Froude scaling laws to aerodynamic parameters and ensure consistency between the components of the system. The geometric scaling factor is defined as λ = 1/50; the scaling of all other parameters needed to model an offshore wind system are derived from this factor such that the three non-dimensional quantities described above are maintained between scales.

To apply Froude scaling, the dimensions of each dependent wind turbine parameter are resolved in terms of three independent parameters: mass, length, and time. According to Froude similitude, mass, length, and time are scaled by factors of λ^3, λ, and $\lambda^{1/2}$, respectively (Martin, 2011; Chakrabarti, 2008). These scaling parameters are elementary and independent, and are the basis for deriving the scaling of all other parameters. A major difference between these scaling laws and those used for downscaling or upscaling of system components to different full-scale sizes is the exclusion of the temporal scaling factor in the latter technique. With the help of dimensional scaling, the scaling laws for various wind turbine parameters were derived in this paper by maintaining a constant Froude number at both scales. Therefore, Froude number at full scale and model scale was equated to obtain the scaling of the quantities that define Froude number (Chakrabarti, 2008), which is the ratio of inertia forces to gravity forces,

$$F_r = \frac{u^2}{gD}. \tag{1}$$

To apply Froude scaling, one can write,

$$(F_r)_{model\ scale} = (F_r)_{full\ scale}. \tag{2}$$

The diameter (length) is scaled by a factor of λ, which states that the full-scale diameter should be 50 times larger than the model-scale diameter. Here, g is not affected by scaling laws because the scaling laws for its numerator (length) and denominator (time)^2 are equal; hence, it becomes a dimensionless quantity for Froude similitude and Eq. 2 can be written as,

$$(u)_{model\ scale} = \lambda^{1/2}\,(u)_{full\ scale}. \tag{3}$$

In Eq. 3, we show that the scaling factor for fluid velocity is derived as $(\lambda)^{1/2}$. The second quantity that is maintained in the DeepCwind scaling laws is consistency of the ratio between wind speed and wave celerity (Martin, 2011). These quantities are measured in the same units (m/s), and thus a consistent value of this ratio ensures proper scaling of forces exerted by wind and wave. This ratio is scaled according to the fundamental scaling laws of Froude scaling. The wind speed to wave celerity ratio is mathematically written as,

$$\alpha = \frac{V}{C}. \tag{4}$$

For this quantity, the mandatory condition is,

$$(\alpha)_{model\ scale} = (\alpha)_{full\ scale}. \tag{5}$$

The third similarity factor of the DeepCwind scaling laws is applied to maintain the consistent rotational characteristics of the wind turbine (Martin, 2011). To ensure this similarity, the tip-speed ratio should be maintained at a constant magnitude. The ratio is mathematically represented as,

$$TSR = \frac{\Omega\, R}{V}. \tag{6}$$

Therefore, for tip-speed ratio similitude, the essential relation is,

$$(TSR)_{model\ scale} = (TSR)_{full\ scale}. \quad (7)$$

On mathematical manipulation of Eqs. 3 and 7, one can derive that the wind speed is reduced by a factor of $\lambda^{1/2}$ and rotor angular speed is increased by a factor of $(1/\lambda)^{1/2}$ when converted from full scale to a model scale. This ratio is derived from fundamental laws of Froude scaling. In Eqs. 4 and 6, the mathematical definitions of tip-speed ratio and wind speed to wave celerity ratio show that these ratios are dependent on parameters that are based on the fundamental scaling parameters; i.e., mass, length, and time. In other words, these ratios cannot be considered as independent scaling laws because they are entirely dependent on Froude scaling. Therefore, for other input parameters (shown in Table 1), we used Froude similitude as the basis of their derivation. For example, the nacelle mass moment of inertia is represented by:

$$J = mr^2. \quad (8)$$

Eq. 8 can be written in a dimensional form as

$$[J] = [mass] \times [length]^2. \quad (9)$$

On equating the nacelle inertia from full-scale and model-scale, one can write:

$$J_{model\ scale} = \Lambda J_{full\ scale}. \quad (10)$$

where Λ is the derived scaling factor for the inertia. We know that from Froude scaling law, the mass is scaled down by a factor of λ^3 where $\lambda = (1/50)$ and radius is scaled down by a factor of λ. Therefore, one can write:

$$\Lambda = (\lambda^3 \times \lambda^2) = \lambda^5. \quad (11)$$

One of the important structural parameters of a FOWT, and thus requires proper scaling, is the bending stiffness. The bending stiffness strongly influences the vibrational response of the system and couples the aerodynamic and hydrodynamic loads exerted on the FOWT. Bending stiffness is mathematically represented as *EI*, which means that its' scaling is dependent on the derived scaling law for Young's Modulus *(E)* and the moment of inertia *(I)*. The derived scaling law for Young's Modulus is λ, and for moment of inertia it is λ^4. Therefore, by applying the derived scaling laws of these quantities to the mathematical formulation of bending stiffness *(EI)*, one can derive the scaling law for bending stiffness as λ^5. Note that while it is important to maintain proper scaling of the bending stiffness, one does not typically maintain proper scaling of the Young's Modulus as it can be difficult to find such a material. Instead, the focus is on maintaining the proper scaling of *EI*; in the DeepCwind project, this was achieved by selecting an appropriate moment of inertia to maintain the λ^5 scaling.

Using the same dimensional-based approach shown in Eqs. 8 through 11, we derived the system parameters for this study shown in Table 1. The following list of parameters is only a part of the list that represents the scaling laws for the rotor-nacelle assembly, tower, platform, aerodynamics, hydrodynamics, and structural dynamics properties of the wind turbine system.

Table 1: Scaling laws for prominent input parameters in FAST code.

Input Parameter	Scaling Law
Total run time and time step	$\lambda^{1/2}$
Generator and rotor angular speed	$\lambda^{-1/2}$
Tower height, tip and hub radius	λ
Nacelle top to center of mass (x) (y) and (z)	λ
Blade, tower, platform, nacelle and hub mass	λ^3
Hub, nacelle and generator mass moment of inertia	λ^5
Blade and tower moment of inertia	λ^4
Blade and tower bending stiffness	λ^5
Tower draft and platform CM from MSL	λ
Displaced Volume of Water	λ^3
Platform diameter, water depth, and wave ht.	λ
Wave peak-spectral period	$\lambda^{1/2}$

SCALING LAW VERIFICATION PROCEDURE

This section gives an overview of the FAST code verification and testing process for the scaling laws that interlink the full-scale and model-scale parameters. Verification of the scaling law accuracy is accomplished through the analysis of two different platform configurations: a modified version of the OC3-Hywind spar-buoy and the MIT/NREL TLP. We call the system analyzed a "modified" version of the OC3-Hywind system because it does not contain the additional stiffness and damping terms used in the OC3 analysis to get the model response to match tank test results performed by Statoil on a scaled Hywind system. Therefore, the simulation results in this paper may not exactly match those of previous OC3-Hywind simulations.

Details about the systems are given in the next section. The process used for verification is described as follows (and depicted in Fig. 1):

1. Full-scale models of the two floating offshore wind systems to be examined are created in FAST.
2. Using the scaling laws, the FAST models are converted to model scale.
3. Simulations are performed at model scale for a variety of load cases.
4. The outputs obtained from the model-scale simulations (forces, displacements) are scaled back up to full scale using the same scaling laws.
5. Simulations are performed using the full-scale model for a variety of load cases.
6. The simulation results from the up-scaled model are then compared to the simulation results from the full-scale model. If the scaling laws are consistent, these results should be the same.

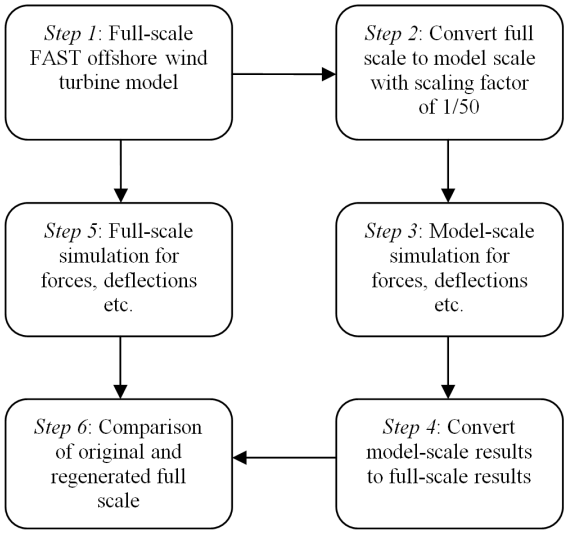

Fig. 1: Flowchart for scaling simulation procedure.

SYSTEM CONFIGURATIONS: TURBINE, PLATFORMS, WIND AND WAVE SPECIFICATIONS

The two platform configurations incorporated and compared in this research for various wind and wave loading tests include: the OC3-Hywind spar-buoy (Jonkman, 2009a) and the NREL/MIT TLP (Matha, 2010). The systems were chosen due to the diversity in design and mooring configuration and therefore, response characteristics. Details on the design specifications for these platforms are given below in Table 2 and Fig. 2:

Table 2: Structural and hydrodynamic properties of platform configurations.

Properties	TLP	Spar-buoy
Tower Freeboard from MSL	0	10 m
Center of Mass (Platform) from MSL (Positive Downward)	40.612 m	89.9155 m
Platform Mass	8600410 kg	7466330 kg
Water Displaced in a Still Water Condition	12179.60 m^3	8029.21 m^3
Platform Diameter	18 m	6.5 m
Coefficient of Drag	0.6	0.6

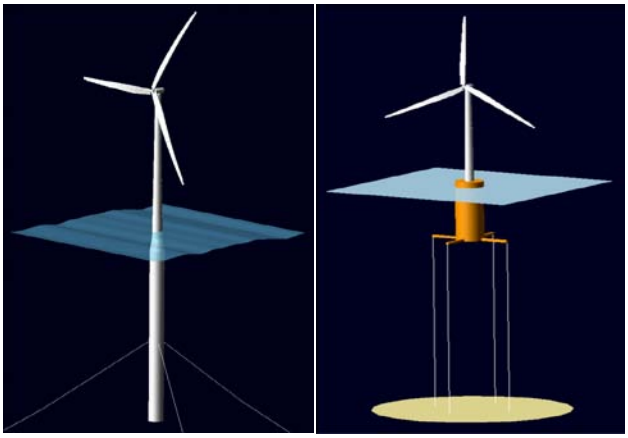

Fig. 2: Sketches of OC3-Hywind spar-buoy (left) and NREL/MIT TLP (right).

The turbine used for this research is the 5-MW reference wind turbine from NREL, which is a three-bladed, upwind turbine. The design of this turbine is a reinvention inspired from the technical specifications of Multibrid M5000, REpower 5M, WindPACT, RECOFF and DOWEC wind turbines (Jonkman et. al., 2009b). Some of the properties of the turbine are stated below:

Table 3: Structural and aerodynamic properties of 5-MW wind turbine.

Structural and Aerodynamic Properties	Numerical Value
Tip Radius	63 m
Hub Radius	1.5 m
Tower Height	87.6 m
Rotor Pre-cone Angle	2.5 deg
Nacelle Mass	240000 kg
Hub Mass	56780 kg

Simulated wind files are generated by using NREL's TurbSim code (Jonkman, 2009), which generates turbulent wind files to evaluate turbine response in various wind conditions. Wave effects are simulated using HydroDyn (Jonkman, 2007a), which generates the hydrodynamic forces and loads using WAMIT (WAMIT Inc., 1998) as a preprocessor for defining the hydrodynamic coefficients of the platform. HydroDyn simulates loads and forces for periodic (consistent amplitude and frequency) and irregular waves. Periodic waves are simulated by using Airy wave theory and nonperiodic waves are generated according to JONSWAP/Pierson-Moskowitz spectra (Jonkman, 2007a). Predetermined wave conditions for these functions are defined in input files in terms of water density, water depth, significant wave height, peak-spectral period and wave direction.

When these scaling laws are applied to the existing wind turbine and offshore floating platform designs, new input files are created for FAST using MATLAB scripts for maintaining accuracy and consistency. FAST v7.00.01a-bjj is applied in all simulations (Jonkman et. al., 2005).

ASSUMPTIONS

For standardization of scaling law simulations, we created and followed a few assumptions that are applied to all test procedures demonstrated in this paper. These conditions are described below.

1. Fluid properties such as kinematic viscosity and density for full scale and model scale are equivalent.
2. Parameters that normally would depend on Reynolds number – such as lift and drag coefficients – were left unchanged between full and model scale, which effectively means that Reynolds number was maintained between scales. The turbine was geometrically scaled according to Froude scaling, which assumes consistent lift/drag coefficients, but this does not hold true in a wave tank. This issue will be discussed in subsequent papers.
3. The generator is prescribed to rotate at a constant speed.
4. Blade and tower vibration mode shapes are equivalent for full scale and model scale.
5. The control module is inactive in the simulations. Therefore, control algorithm bound parameters such as pitch and yaw angle are either zero or maintained at a constant value for different wind and wave loading conditions.
6. The standard simulation time is assumed to be 630 seconds.
7. Material densities are equivalent, but the stiffnesses are scaled between full scale and model scale.
8. The wind and waves are aligned.
9. The rotor angular speed was scaled according to Froude scaling, which means that the once-per-rev (1P), three-per-rev (3P) and other rotor harmonic frequencies are scaled according to Froude scaling as well.

RESULTS AND DISCUSSION

To examine the similarity in system performance between full scale and model scale, we conducted simulations with a variety of loading conditions. The simulations that were run (conducted for both platform configurations) are divided into six categories, as described below.

1. *Static analysis:* The first simulation that was performed is a static analysis to ensure that the mass, buoyancy and mooring pretension of the system are balanced, and therefore are scaled appropriately.
2. *Free-decay tests with initial offsets*: In these tests, the decay pattern is examined to compare structural frequencies and damping characteristics of the systems. Wind and waves are not used in these simulations.
3. *Steady wind and still water:* These tests are conducted to characterize structural response of the system from wind loads only. Wave conditions are ignored in this category. A steady wind at 8 m/s and

1.13 m/s for full scale and model scale, respectively, is used with zero vertical and horizontal wind shear. In addition to wind speed, rotor speed is set at 9 rpm and 63.63 rpm for full scale and model scale respectively, according to specifications given for the 5-MW wind turbine design.

4. *Still air and periodic waves:* These tests are conducted for assessment of system response to wave-induced loads only. Wind conditions are ignored in this category. Periodic wave conditions include wave height, which is 6 m and 0.12 m, for full scale and model scale respectively; and wave period, which is 10 s and 1.41 s for full scale and model scale, respectively.
5. *Steady wind and periodic waves*: In these tests, both aerodynamic and hydrodynamic excitations are included in the simulations. The wind speed, wave height, wave period, and rotor speed are the same as from steps 3 and 4.
6. *Turbulent wind and irregular waves*: This category of tests is very significant to analyze system response as it represents a complicated stochastic wind/wave loading scenario. The turbulent wind is averaged at 8 m/s at full scale and 1.13 m/s at model scale; with a turbulence intensity of 40%. The waves are irregular with a mean significant wave height of 6 m and 0.12 m and peak spectral wave period of 10 s and 1.41 s for full scale and model scale, respectively. As stated earlier, the rotor rpm is kept consistent at 9 rpm and 63.63 rpm for full scale and model scale, respectively, with stochastic wind and wave loads.

In these test conditions (except static analysis and free-decay tests), the steady wind condition is maintained at a constant wind speed of 8 m/s and the turbulent wind condition has a mean wind speed of 8 m/s. We chose these wind speed values because the wind turbine control module was inactive in our simulations and we therefore wanted to stay in the region of the power curve between cut-in and rated wind speed where control is less important. We conducted the tests independently on both full-scale and model-scale configurations. The output parameters calculated by FAST were very extensive and therefore only a limited number of parameters were analyzed to ensure similar results. The output parameters analyzed include:

1. *Blades*: loads at the base, and in-plane and out-of-plane deflections at the tip.
2. *Tower*: tower-top shear and axial forces; and bending moments.
3. *Platform*: 6-DOF motion of the platform, and loads at the connection point between the platform and tower (tower base).
4. *Mooring Lines*: fairlead and anchor tensions.

These parameters will be used to assess the full-scale and model-scale compliance. The scaling factors for these parameters between full and model scale are given in Table 4. These factors are also based on Froude scaling.

Table 4: Scaling laws for relevant output parameters in FAST code.

Output Parameter	Scaling
Blade tip deflections	λ
Tower Shear Forces	λ^3
Tower Bending Moments	λ^4
Platform Translational Displacements	λ
Mooring Line Tensions	λ^3

The comparison between full and model scale is excellent. Therefore, only the most complicated simulations with turbulent wind and irregular waves are reviewed in this paper. In Fig. 3, the time histories of the turbulent wind speed at the hub and the wave elevation of the irregular waves at the undisplaced platform centerline used in these simulations are shown. These values are helpful in understanding the perturbations related to forces, moments, and motions of different structural components shown in Figs. 4 through 11. The wind speed reaches roughly 17 m/s for full scale and 2.4 m/s for model scale, respectively. The wave elevation attains a maximum value of approximately 5 m above and below the platform. These conditions are quite stochastic and represent a rigorous wind/wave loading scenario that is useful for scaling law verification. The output parameters from the turbulent wind and irregular wave simulations at both scales are shown in Figs. 4, 6, 8 and 10 for the spar-buoy platform; and Figs. 5, 7, 9 and 11 for the TLP. Full-scale and model-scale results for spar-buoy platform are plotted together by blue and red lines, respectively; and full-scale and model-scale outputs for TLP are exhibited together by red and blue lines, respectively. The model-scale outputs are scaled to full scale in the figures.

Figs. 4 and 5 show that the out-of-plane and in-plane blade tip deflections almost perfectly coincide with each other. In Figs. 4 through 11, the time histories of all the displacements, forces and deflections do not die out with increasing time, which is happening due to the continuous excitation by turbulent wind at a mean value of 8 m/s (full scale) and 1.13m/s (model scale); and irregular wave with a peak-spectral period of 10 s and 1.41 s and a significant wave height of 6 m and 0.12 m at full scale and model scale, respectively.

The shear and axial forces, and bending moment trends for tower top/yaw bearing are quite different among the selected platform configurations. In Fig. 6 (spar-buoy configuration), it is observed that the tower-top fore-aft shear force reaches a maximum of approximately 1600N while the same shear force regime is limited to 1200N roughly for the TLP configuration (Fig. 7). Similar differences have been observed for side-to-side and vertical force between spar-buoy and TLP systems, where TLP systems have more constrained displacements and rotations as compared to a spar-buoy platform. It is important to note here that although the system properties (Tables 2 and 3) are completely different for both configurations; their structural response is consistent when compared between a full-scale and a model-scale system.

The platform translational and rotational motions were further analyzed to ensure similarity in the hydrodynamic loading between the full-scale and model-scale system. Figs. 8 and 9 show that surge, sway, and heave displacements for the spar-buoy platform are much higher in magnitude when compared to the TLP system. A similar pattern is documented for differences between the rotational displacements of the two platform configurations. The restricted displacement characteristics result from the added pretension in the mooring lines of the TLP system that is not present in the slack mooring lines of a spar-buoy system. This reasoning is further supported by the elevated downwind mooring line tensions of up to 6,000 N for a TLP system shown in Fig. 11 with a higher frequency of perturbations as compared to the spar-buoy system (Fig. 10). Moreover, the underlying fact that can be summarized from these results is that the hydrodynamic similitude requirements of different platform systems have been met by the scaling laws applied in this research.

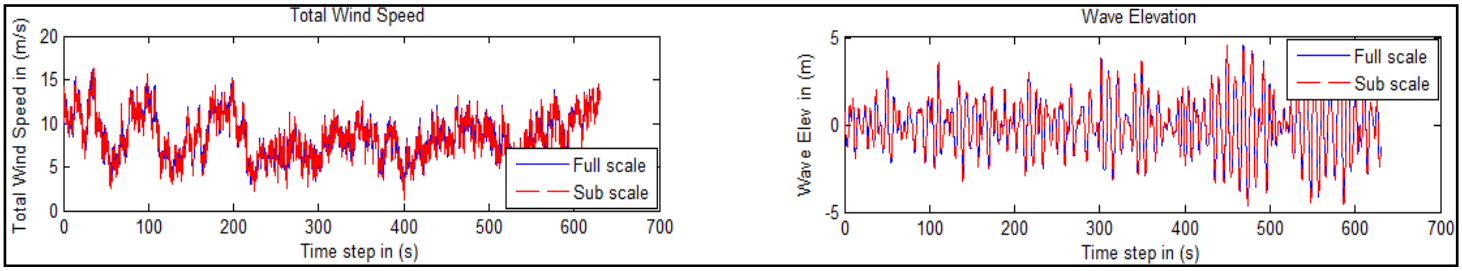

Fig. 3: Time history of total turbulent wind speed and wave elevation of irregular waves, for both OC3-Hywind and MIT/NREL TLP system.

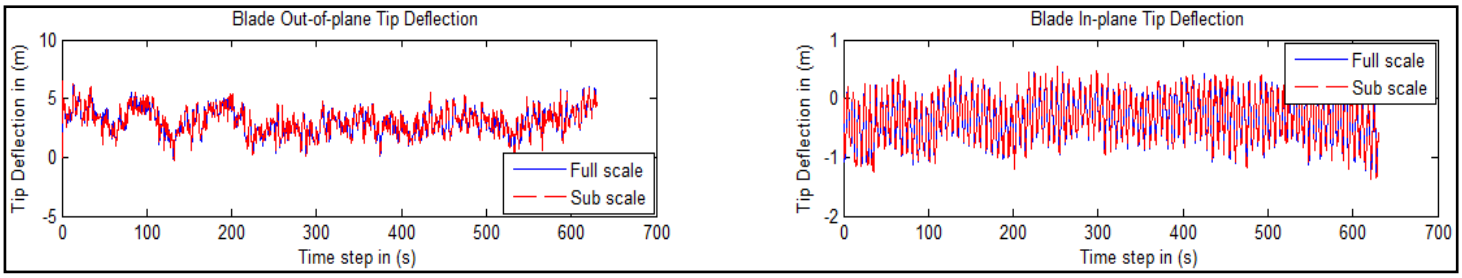

Fig. 4: Time history of blade tip out-of-plane and in-plane deflection for the turbine supported by OC3-Hywind spar-buoy platform.

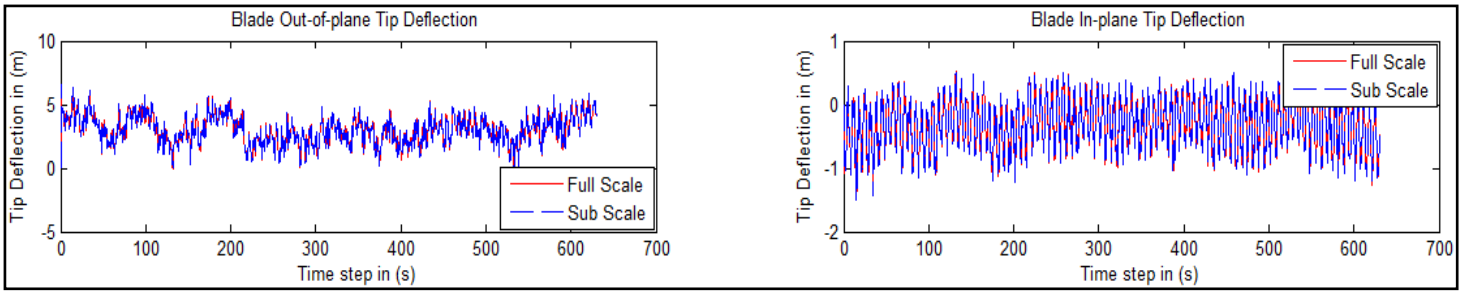

Fig. 5: Time history of blade tip out-of-plane and in-plane deflection for the turbine supported by MIT/NREL TLP.

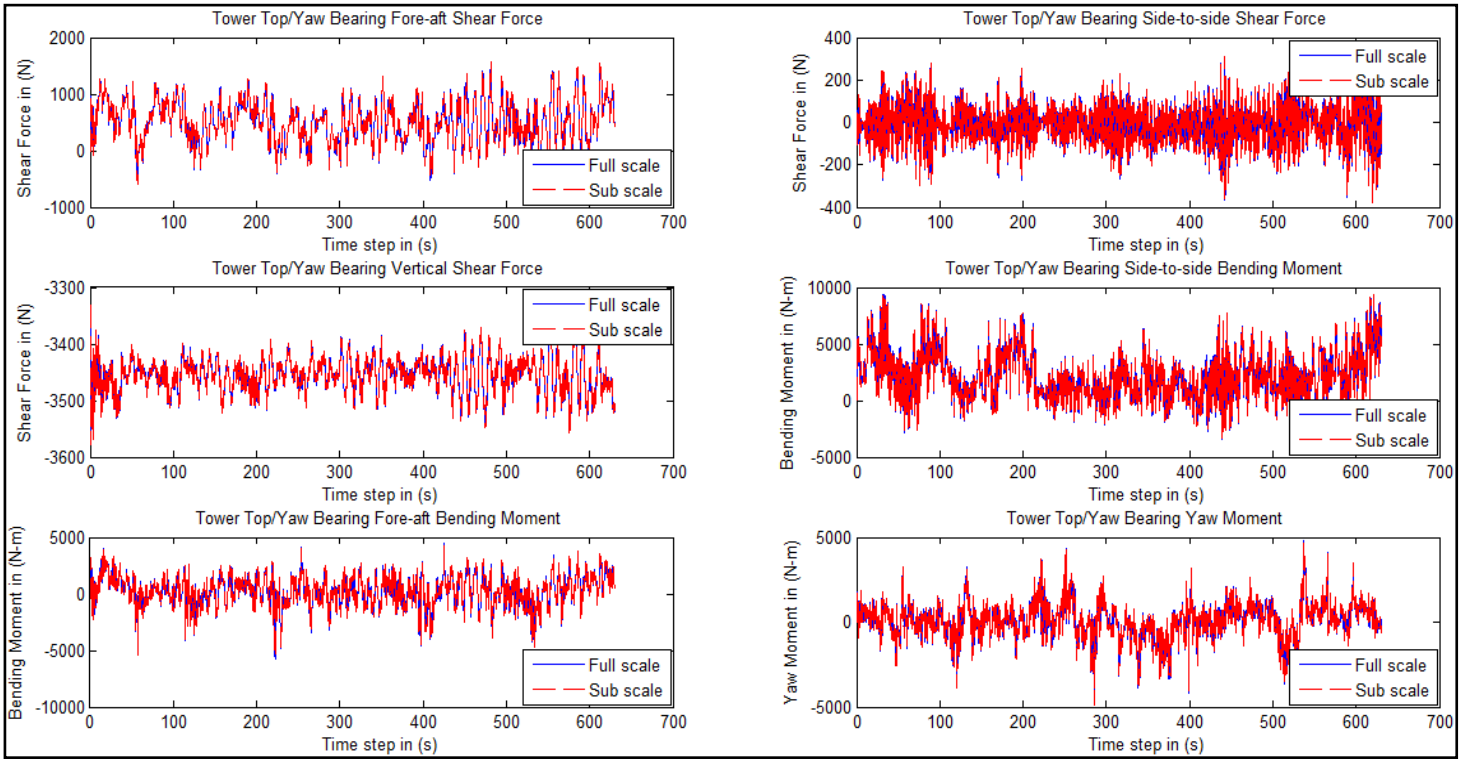

Fig. 6: Time history of tower top/yaw bearing shear and axial forces; and bending moments for OC3-Hywind spar-buoy platform.

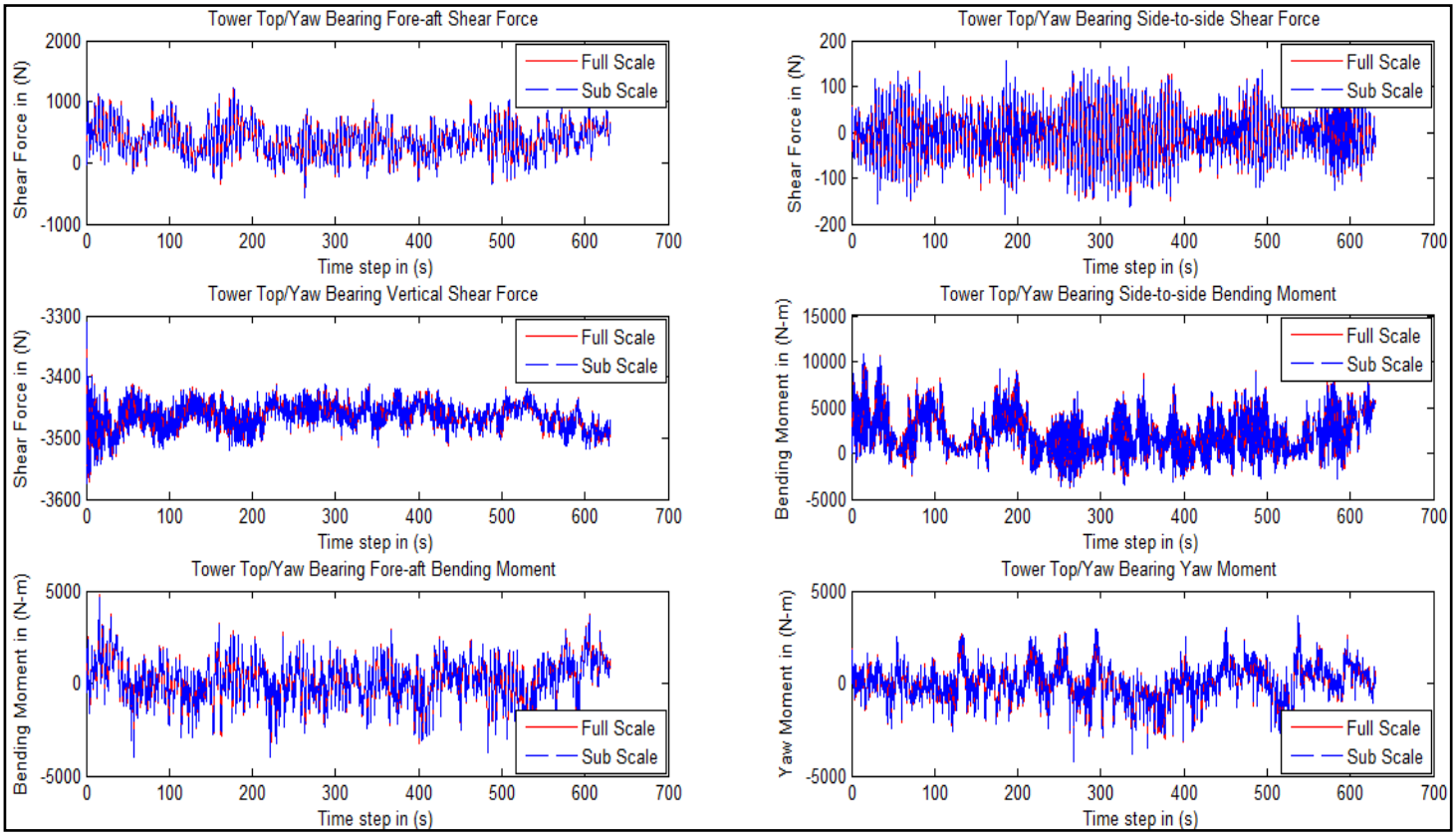

Fig. 7: Time history of tower top/yaw bearing shear and axial forces, and bending moments for MIT/NREL TLP system.

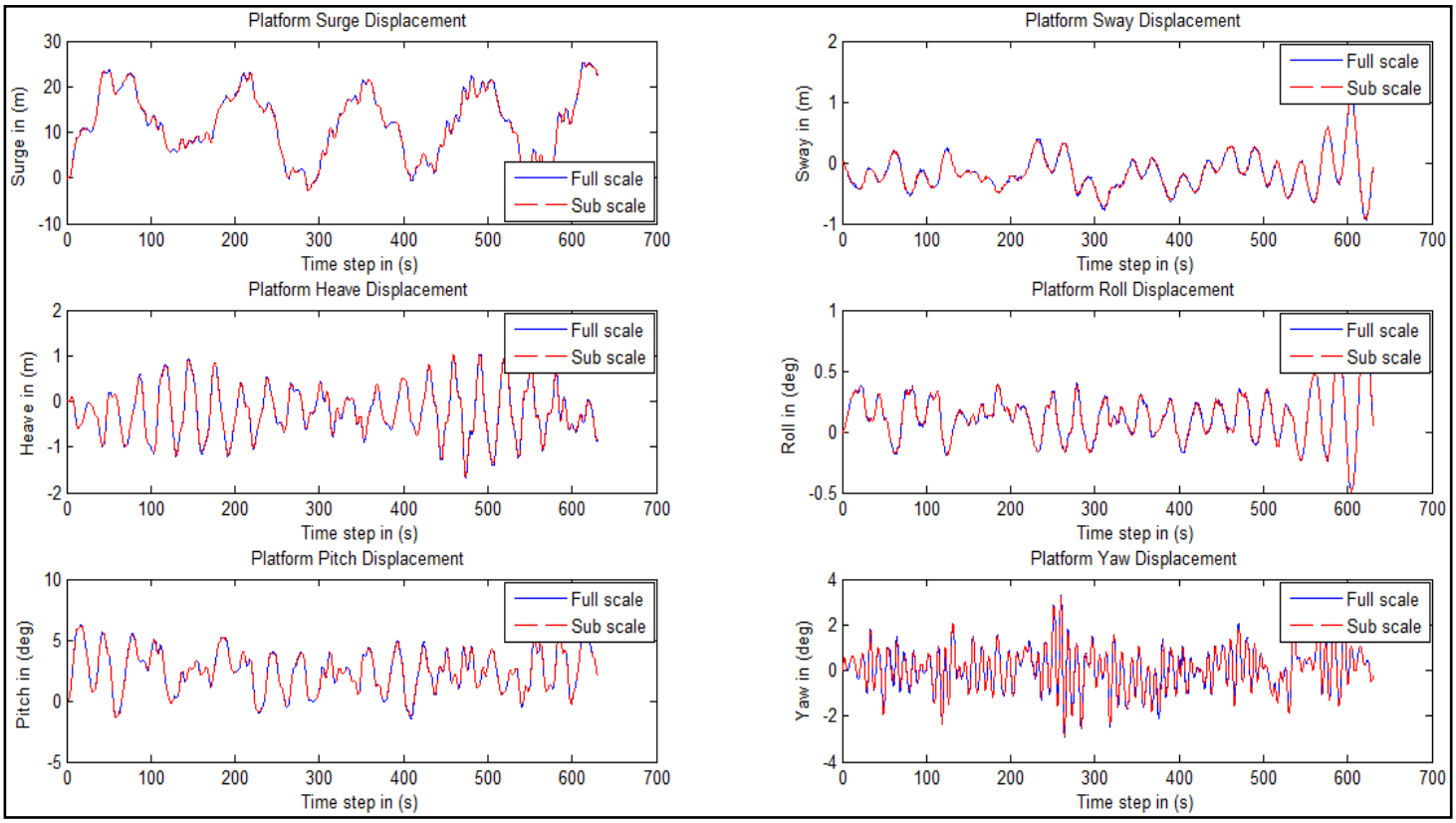

Fig. 8: Time history of platform translational and rotational motions for OC3-Hywind spar-buoy platform.

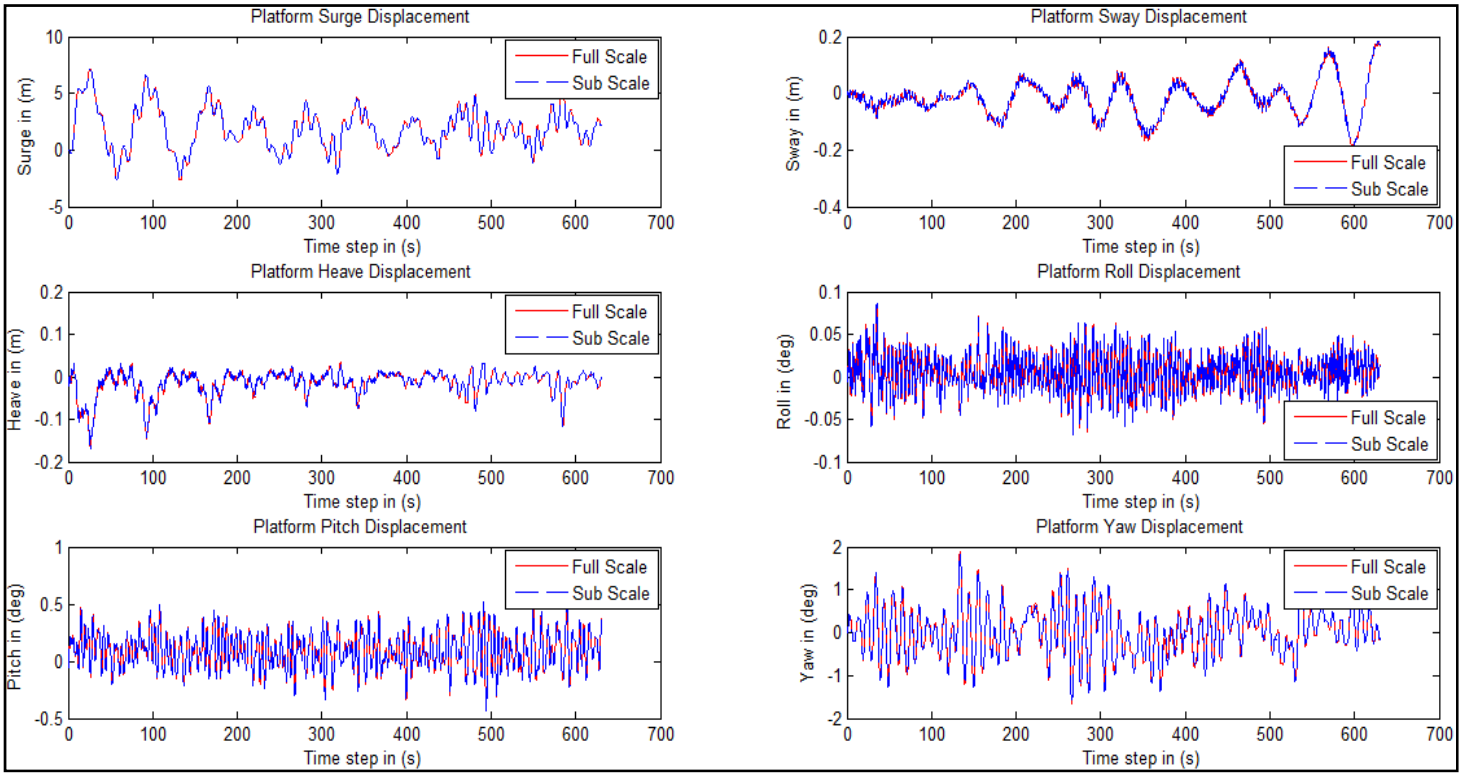

Fig. 9: Time history of platform translational and rotational motions for MIT/NREL TLP system.

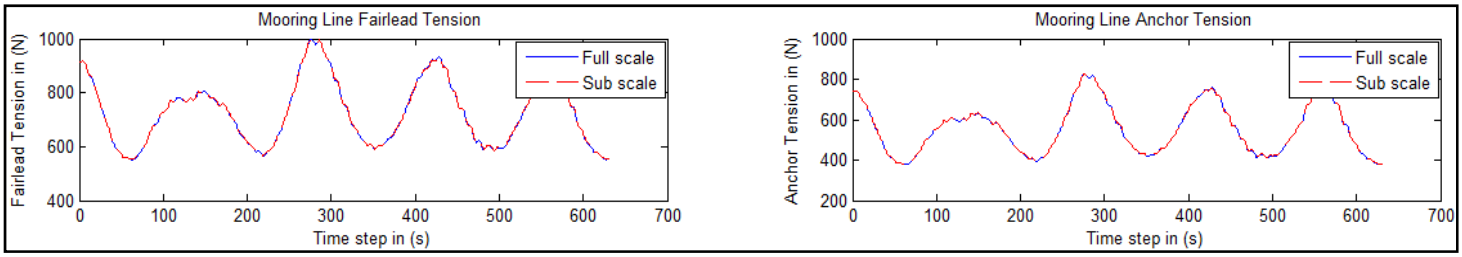

Fig. 10: Time history of downwind mooring line fairlead and anchor tension for OC3-Hywind spar-buoy platform.

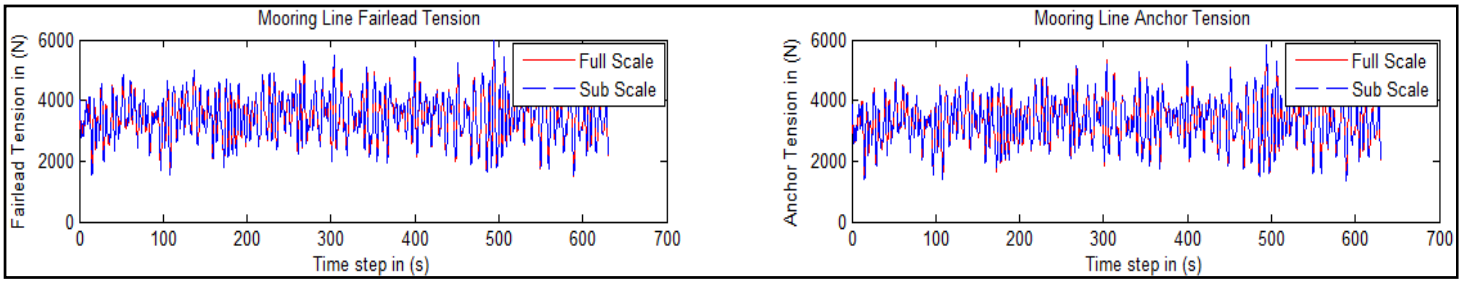

Fig. 11: Time history of downwind mooring line fairlead and anchor tension for MIT/NREL TLP system.

Scaling Verification of Nonlinear Equations

Two examples related to the nonlinear and multi-physics equations of FAST are given here as case studies to further demonstrate the validity of the scaling laws.

The first example is based on the classical Bernoulli-Euler beam theory of a rotating beam and examines the scaling of the elastic stiffness and centrifugal stiffness (two different physical phenomena) of the blades (Jonkman, 2003). The out-of-plane movement of the blade is given by Eq. 12.

$$\underbrace{\frac{\partial^2}{\partial z^2}\left[EI(z)\frac{\partial^2 u(z,t)}{\partial z^2}\right]}_{1^{st}\ term} - \underbrace{\Omega^2\frac{\partial}{\partial z}\left[\int_z^R \rho A(z')\,z'\,dz'\,\frac{\partial u(z,t)}{\partial z}\right]}_{2^{nd}\ term} + \underbrace{\rho A(z)\frac{\partial^2 u(z,t)}{\partial t^2}}_{3^{rd}\ term} = 0. \tag{12}$$

There are three terms in Eq. 12 and by applying Froude scaling laws to each individual term; they can be rewritten in a dimensional form as,

First term (when the overall bending stiffness *EI* is scaled appropriately):

$$\left[\frac{1}{\lambda^2}\right] \times \left[\lambda^5 \left(\frac{\lambda}{\lambda^2}\right)\right] = \lambda^2. \tag{13-a}$$

Second term:

$$\left[\left(\frac{1}{\lambda^{1/2}}\right)\right]^2 \times \left(\frac{1}{\lambda}\right)\left[(\lambda^2 \times \lambda \times \lambda)\left(\frac{\lambda}{\lambda}\right)\right] = \lambda^2. \tag{13-b}$$

Third term:

$$\lambda^2 \times \left[\frac{\lambda}{(\lambda^{1/2})^2}\right] = \lambda^2. \tag{13-c}$$

Eqs. 13-a through 13-c, show that the individual terms in Eq. 12 have consistent scaling factors when Froude scaling laws are applied. Therefore, it is concluded that a nonlinear partial differential equation that defines the characteristic motion (natural mode shapes and frequencies) of a rotating blade is in agreement between a full-scale and model-scale wind turbine design.

The second example (Eqs. 14 and 15) examines the strong nonlinearity related to catenary mooring line force-displacement relationships by showing equations that represent horizontal and vertical force-displacement relationships between the fairlead and anchor of the catenary mooring lines as implemented in FAST (Jonkman et. al., 2007b). These relationships account for the buoyancy, elastic stretching, seabed interaction, and nonlinear geometry of the catenary moorings.

$$x_F(H_F, V_F) = \underbrace{L}_{1^{st}\,term} - \underbrace{\left[\frac{V_F}{\omega}\right]}_{2^{nd}\,term} + \underbrace{\frac{H_F}{\omega} ln\left[\frac{V_F}{H_F} + \sqrt{1 + \left(\frac{V_F}{H_F}\right)^2}\right]}_{3^{rd}\,term} + \underbrace{\left[\frac{H_F L}{EA}\right]}_{4^{th}\,term} +$$

$$\underbrace{\frac{C_B \omega}{2EA}\left[-\left(L - \frac{V_F}{\omega}\right)^2 + \left(L - \frac{V_F}{\omega} - \frac{H_F}{C_B \omega}\right) MAX\left(L - \frac{V_F}{\omega} - \frac{H_F}{C_B \omega}, 0\right)\right]}_{5^{th}\,term}. \tag{14}$$

and,

$$z_F(H_F, V_F) = \underbrace{\frac{H_F}{\omega}\left[\sqrt{1 + \left(\frac{V_F}{H_F}\right)^2} + 1\right]}_{1^{st}\,term} + \underbrace{\left[\frac{V_F^2}{2EA\omega}\right]}_{2^{nd}\,term}. \tag{15}$$

In Eqs. 14 and 15, the vertical and horizontal distances are scaled by a factor of λ, according to the Froude similitude. By applying Froude scaling laws on the right side of these equations, we can prove that the equations follow Froude scaling. There are five terms in Eq. 14 and by applying Froude scaling laws to each individual term in these equations, one can write them in a dimensional form as,

First term:

$$\lambda = \lambda. \tag{16-a}$$

Second term:

$$\frac{\lambda^3}{\lambda^2} = \lambda. \tag{16-b}$$

Third term:

$$\frac{\lambda^3}{\lambda^2}\left[\frac{\lambda^3}{\lambda^3} + \sqrt{\left(\frac{\lambda^3}{\lambda^3}\right)^2}\right] = \lambda. \tag{16-c}$$

Fourth Term:

$$\frac{\lambda^3 \lambda}{\lambda^3} = \lambda. \tag{16-d}$$

Fifth Term:

$$\frac{\lambda^2}{\lambda^3}\left[-\left(\lambda - \frac{\lambda^3}{\lambda^2}\right)^2 + \left(\lambda - \frac{\lambda^3}{\lambda^2} - \frac{\lambda^3}{\lambda^2}\right) \times \left(\lambda - \frac{\lambda^3}{\lambda^2} - \frac{\lambda^3}{\lambda^2}\right)\right] = \lambda. \tag{16-e}$$

and, the two individual λ terms in Eq. 15 can be written in the dimensional form as,

First term:

$$\frac{\lambda^3}{\lambda^2}\left[\sqrt{\left(\frac{\lambda^3}{\lambda^3}\right)^2}\right] = \lambda. \tag{17-a}$$

Second term:

$$\frac{(\lambda^3)^2}{\lambda^3 \lambda^2} = \lambda. \tag{17-b}$$

It is shown in Eqs. 16-a through 17-b that individual λ terms on the right side combine into a resultant λ, which is equal to the scaling law for x_F and z_F representing the distances related to fairlead and anchor points. Therefore, it shows that Froude scaling remains valid for Eqs. 14 and 15.

Drawback of Froude Scaling

In a typical offshore floating system, Froude scaling and Reynolds scaling models cannot be applied simultaneously. This incompatibility between the scaling models is one of the reasons behind discrepancies in the system response of a model-scale floating wind turbine and its corresponding full-scale prototype. The assumptions we made in this paper mitigate such differences between both the scales that makes our simulation results different from system responses obtained from a typical offshore wind system experiment. In other words, we were able to avoid the Reynolds number mismatch within the simulation by keeping the Reynolds number-dependent parameters consistent between the full-scale and model-scale simulations; i.e., the airfoil lift and drag coefficients and viscous damping.

Moreover, viscous damping is increased for a model-scale system as compared to its corresponding full-scale system in the case of physical model testing because Reynolds number is reduced by a factor of $\lambda^{3/2}$ (Froude scaling effect). Reynolds number is the ratio of inertial forces to viscous forces, so a decrease in this value means an increase in viscous forces. The above explanation leads to the conclusion that the results shown above (Figs. 3 ~ 11) should not match for physical model testing. But, in our simulations the viscous damping is consistent because Reynolds's number dependent quantities (stated above) are assumed to be constant for both full-scale and model-scale systems.

This will not hold true for a real model-scale test, where Reynolds number will change and thus alter the viscous damping. These scaling effects have been discussed in other research papers (Martin, 2011; Goupee et. al., 2012; Stewart et. al., 2012) from the DeepCwind consortium.

As stated earlier, Reynolds number equivalence is not maintainable when Froude scaling is used for model-scale testing (Chakrabarti, 2008; Martin, 2011). Additionally, it becomes extremely challenging to ignore its effects when the model is scaled by a high factor such as 1/50, which was used in the DeepCwind model testing. Therefore, we further examined the Reynolds number scaling effects. The Reynolds number, which is the ratio of inertial forces to viscous forces, is mathematically expressed by,

$$Re = \frac{uD}{\nu}. \tag{18}$$

For Reynolds number similitude, it is desirable that this dimensionless number be consistent for both scales (Chakrabarti, 2008; Martin, 2011). But, when Froude scaling laws are applied to Reynolds number, inaccurate results are obtained, which are shown below:

$$(Re)_{model\ scale} = (Re)_{full\ scale}. \tag{19}$$

$$\left(\frac{uD}{\nu}\right)_{model\ scale} = \left(\frac{uD}{\nu}\right)_{full\ scale}. \tag{20}$$

Using Froude scaling and the fact that the fluid is unchanged between full and model scale, Eq. 20 is rewritten as:

$$(Re)_{model\ scale} = \lambda^{3/2}(Re)_{full\ scale}. \tag{21}$$

Eq. 21 is a result of Froude scaling but is considered as incorrect according to Reynolds scaling (Eq. 19) and defines the issue of discontinuity between the two models (Chakrabarti, 2008; Martin, 2011). In our case, the fundamental scaling factor λ is 1/50 and therefore the Reynolds number for a practical model test becomes $(1/50)^{3/2}$ in the case of Froude scaling. To minimize this effect, the fluid used for model tests ideally would have elevated turbulence to match the damping effects emerging due to variation in Reynolds number (Chakrabarti, 2008). Such modifications in the fluid and structure interaction are quite challenging for model or prototype testing. On the other hand, this situation is easily avoided in the simulations conducted in FAST, where we have assumed the physical quantities that are strongly dependent on Reynolds number, are constant for full scale and model scale.

The effect of Reynolds number could be included in this research by following Eq. 21 and reducing the Reynolds number by a factor of $\lambda^{3/2}$. But, this effort would not serve the purpose of this paper which is to verify the scaling laws used in the DeepCwind model testing using the FAST code.

As stated earlier, we are developing companion papers where the model tests and FAST results are compared. This first step was needed to understand if comparing full-scale simulations to up-scaled results from the tank could be done in a consistent manner. In fact, during this process we learned of parameters in the modeling tool that needed to be scaled, and weren't initially identified. This work was a sanity check for going forward with model validation activities, using the offshore wind modeling tool, FAST.

CONCLUSIONS

In this paper, we explained the motivation behind the need to develop and verify scaling laws for offshore wind turbines using the FAST code. The necessary similitudes of Froude scaling (and subsequently, tip-speed ratio and wind speed to wave celerity ratio) are maintained throughout all the simulations performed in this work. We performed parallel simulations for full scale and model scale and then transformed the model scale outputs back to full scale to compare and show that requirements of the aforementioned scaling laws are met. We demonstrated the Froude scaling technique for generating scaling laws for different physical quantities that are used for modeling a wind turbine in FAST.

We used two different platform configurations—the OC3-Hywind spar-buoy and the MIT/NREL TLP—in our simulations. Both systems exhibit different structural and hydrodynamic properties and were selected for our research to ensure the validity of the scaling laws for various offshore wind systems. We described our testing procedure, which consists of different wind-wave conditions to characterize the response exhibited by different structural components of an offshore wind turbine with special focus on platform and mooring line configuration. When the output parameters for both platform configurations were compared, we found that all the full-scale and model-scale quantities were in excellent agreement with the scaling laws. The excellent agreement between the full-scale and model-scale output parameters exists because both Froude number (Eq. 1) and Reynolds number (Eq. 18) are kept constant between full scale and model scale simulations. Such consistency is impossible to achieve in physical tests, and a large scaling factor between full scale and model scale further adds to the challenges because Reynolds number distortion increases with increasing fundamental scaling factor, by an exponential factor of 3/2 (as shown in Eq. 21).

With the help of nonlinear equations that represent the characteristics of a rotating blade and catenary mooring line force-displacement relationships, we verified successful application of Froude scaling to such complex relations, as shown in Eqs. 12 through 17-b. Therefore, we have shown through FAST simulations that the scaling laws adopted by the DeepCwind project are an appropriate approach for performing scaled model tests with the exception of Reynolds number issues.

REFERENCES

Chakrabarti, Subrata K. (2008). *The Theory and Practice of Hydrodynamics and Vibration*, World Scientific: Singapore, Advanced Series on Ocean Engineering, Vol. 20.

Cermelli, C., Aubault, A., Roddier, D., McCoy, T. (2010). *Qualification of a Semi-Submersible Floating Foundation for Multi-Megawatt Wind Turbines,* Offshore Technology Conference, Texas, USA, OTC: OTC-20674-PP.

De Ridder, E. J., Koop, A., Doeveren, B. (2011). *DeepCwind Floating Wind Turbine Model Tests*, Maritime Research Institute, The Netherlands, Report No. : 24602-1-OB, Vol. 1.

Goupee, Andrew J., Koo, Bonjun J., Lambrakos, Kostas F., Kimball, Richard W. (2012). *Model Tests for Three Floating Wind Turbine Concepts,* Offshore Technology Conference, Texas, USA, OTC: OTC-23470-PP.

Jonkman, Jason M., Buhl Jr., Marshall L. (2005). *FAST User's Guide*, National Renewable Energy Laboratory, Golden, Colorado USA, Technical Report: NREL/EL-500-38230.

Jonkman, Jason M. (2007a). *Dynamics Modeling and Loads Analysis of an Offshore Floating Wind Turbine*, National Renewable Energy Laboratory, Golden, Colorado, USA, Technical Report: NREL/TP-500-41958.

Jonkman, Jason M., Jr. Buhl, Marshall L. (2007b). *Development and Verification of a Fully Coupled Simulator for Offshore Wind Turbines*, National Renewable Energy Laboratory, Golden, Colorado, USA, Conference Paper (45th AIAA Aerospace Sciences Meeting and Exhibit, Wind Energy Symposium, USA): NREL/CP-500-40979.

Jonkman, Jason M. (2003). *Analytical Determination of Vibration Modes for Rotating Beams*, University of Colorado at Boulder, USA.

Jonkman, Jason M. (2009a). *Definition of the Floating System for Phase IV of OC3*, Golden, Colorado, National Renewable Energy Laboratory, USA Technical Report: NREL/TP-500-47535.

Jonkman, Jason M., Butterfield, S., Musial, W., Scott, G. (2009b). *Definition of a 5-MW Reference Wind Turbine for Offshore System Development*, National Renewable Energy Laboratory, Golden, Colorado, USA, Technical Report: NREL/TP-500-38060.

Jonkman, B. J. (2009). *TurbSim User's Guide: Version 1.50*, National Renewable Energy Laboratory, Golden, Colorado, USA, Technical Report: NREL/TP-500-46198.

Matha, D. (2010). *Model Development and Loads Analysis of an Offshore Wind Turbine on a Tension Leg platform, with a Comparison to Other Floating Turbine Concepts*, National Renewable Energy Laboratory, Golden, Colorado, USA, Subcontract Report: NREL/SR-500-45891.

Martin, H.R., (2011). *Development of a scale model wind turbine for testing of offshore floating wind turbine systems*, M.S. Thesis, University of Maine, Maine.

Skaare, B., Hanson, T. D., Nielsen, F. G., Yttervik, R., Hansen, A. M., Thomsen, K., Larsen, T. J. (2007). *Integrated Dynamic Analysis of Floating Offshore Wind Turbines,* Hydro Oil and Energy, Norway and Riso National Laboratory, Denmark.

Stewart, Gordon M., Lackner, Matthew A., Robertson, Amy N., Jonkman, Jason M., Goupee, Andrew J. (2012). *Calibration and Validation of a FAST Floating Wind Turbine Model of the DeepCwind Scaled Tension-Leg Platform*, ISOPE 2012, Rhodes, Greece, USA.

(1998-2006). *WAMIT USER MANUAL: Versions 6.4, 6.4PC, 6.3S, 6.3S-PC*, WAMIT Inc., USA.

(2006-2010). *WindSea: Next Generation Floating Wind Farm,* WindSea AS, Sandvika, Norway.